Fabrication of folic acid sensor based on the Cu doped SnO_2 nanoparticles modified glassy carbon electrode

2014 Nanotechnology 25 295501

(http://iopscience.iop.org/0957-4484/25/29/295501)

IOP Publishing Nanotechnology
Nanotechnology **25** (2014) 295501 (9pp) doi:10.1088/0957-4484/25/29/295501

Fabrication of folic acid sensor based on the Cu doped SnO_2 nanoparticles modified glassy carbon electrode

N Lavanya[1], S Radhakrishnan[1], N Sudhan[1], C Sekar[1], S G Leonardi[2], C Cannilla[3] and G Neri[2]

[1] Department of Bioelectronics and Biosensors, Alagappa University, Karaikudi-630 003, Tamilnadu, India
[2] Department of Industrial Chemistry and Materials Engineering, University of Messina, 98166 Messina, Italy
[3] CNR-ITAE, Institute of Advanced Technologies for Energy 'Nicola Giordano', 98126 Messina, Italy

E-mail: sekar2025@gmail.com

Received 3 February 2014, revised 7 May 2014
Accepted for publication 21 May 2014
Published 1 July 2014

Abstract

A novel folic acid biosensor has been fabricated using Cu doped SnO_2 nanoparticles (NPs) synthesized by a simple microwave irradiation method. Powder XRD and TEM studies confirmed that both the pure and Cu doped SnO_2 (Cu: 0, 10, 20wt%) crystallized in tetragonal rutile-type structure with spherical morphology. The average crystallite size of pure SnO_2 was estimated to be around 16 nm. Upon doping, the crystallite sizes decreased to 9 nm and 5 nm for 10 and 20wt% Cu doped SnO_2 respectively. XPS studies confirmed the electronic state of Sn and Cu to be 4+ and 2+ respectively. Cu (20wt%) doped SnO_2 NPs are proved to be a good sensing element for the determination of folic acid (FA). Cu-SnO_2 NPs (20wt%) modified glassy carbon electrode (GCE) exhibited the lowest detection limit of 0.024 nM over a wide folic acid concentration range of 1.0×10^{-10} to 6.7×10^{-5} M at physiological pH of 7.0. The fabricated sensor is highly selective towards the determination of FA even in the presence of a 100 fold excess of common interferent ascorbic acid. The sensor proved to be useful for the estimation of FA content in pharmaceutical sample with satisfactory recovery.

Keywords: Cu doped SnO_2 NPs, x-ray photoelectron spectroscopy, folic acid sensor, differential pulse voltammetry, pharmaceutical products

(Some figures may appear in colour only in the online journal)

1. Introduction

Folic acid (Vitamin B9), a water soluble vitamin, is a very significant compound for normal human metabolic function. Its deficiency in human beings causes different diseases such as gigantocytic anemia, mental devolution, leucopoenia, colon cancer, heart attack and congential malformation. Also, the folic acid (FA) is important for synthesis of DNA and RNA which are primary events for cell growth and division and it is one of the essential coenzymes of the haematopoietic system which controls the formation of ferrohaeme [1, 2]. Therefore, it is of great importance to monitor FA accurately in pharmaceutical and food samples. A wide variety of analytical techniques such as high performance liquid chromatography (HPLC), colorimetry, spectrophotometry, fluorometric, chemiluminescence and microbial methods have been reported for the determination of FA [3–8]. Some of these methods are unsuitable for routine analysis in food industries due to their expensive equipments, time consuming and complicated analytical processes. Hence it is of great significance to develop sensitive and simple method for FA detection. Electrochemical sensors have attracted wide attention due to their facile fabricating processes, low cost, high sensitivity, selectivity, fastness, compatibility and reproducibility. In particular, several FA electrochemical sensors such as salmon sperm dsDNA modified pencil graphite electrode, electrospinning prepared α-Fe_2O_3 nanofiber modified GC electrode, MWCNT/poly(brilliant cresyl blue)

modified GC electrode, SWNT modified GC electrode, etc have been reported [9–12]. Some of these methods involve expensive sensing materials and complex multistep procedures for electrode modification. Hence the low cost material preparation and simple electrode modification protocol with higher electrocatalytic performance for FA is urgently required.

Tin dioxide (SnO_2), a wide band gap (Eg = 3.6 eV) semiconductor with n-type conduction, has been widely used as sensing material in solid state gas sensors [13] due to its outstanding electrical properties accompanied by an elevated chemical stability. However, a very few reports are available concerning the application of SnO_2 for biomolecule detection [14, 15]. The sensing characteristic of SnO_2 can further be improved by chemical doping with appropriate elements (Fe, Cu, Cr, Ni, Co) and/or by preparing composites with carbon nanostructures [16]. Among the transition metal ions, Cu is the most efficient dopant element to improve and tune the electrical, optical and magnetic properties of SnO_2. The substitution of Sn^{4+} (0.74 Å) ions by Cu^{2+} (0.71 Å) ions creates more oxygen vacancies in the SnO_2 system leading to a decrease in the free electron concentration and an optimal doping level is expected to improve the catalytic activity of SnO_2 towards the FA oxidation. Here, we report the synthesis of Cu-doped SnO_2 NPs by a simple microwave irradiation method and its application for the precise determination of folic acid. The Cu-SnO_2 NPs based GC electrode exhibits high sensitivity, excellent selectivity and fast DPV response to the determination of FA which has promising applications in food and pharmaceutical industries.

2. Experimental

2.1. Materials

The reagents used were of analytical grade without further purification; $CuSO_4 \cdot 5H_2O$ and $SnCl_2 \cdot 2H_2O$ (Fischer Scientific, Mumbai) and folic acid (Sisco Research Laboratories, Mumbai). Phosphate buffer (PB) solution (pH 7.0) was prepared using Na_2HPO_4 and NaH_2PO_4. Millipore water was used to prepare the solutions used in the present study.

2.2. Instrumentation

Electrochemical measurements were performed in a conventional two compartment three electrode cell with a mirror polished 3 mm glassy carbon (GC) as the working electrode, Pt wire as the counter electrode and an Ag/AgCl (3 M KCl) as the reference electrode. The electrochemical measurements were carried out with the CHI Model 608D (Austin, TX, USA) electrochemical workstation under nitrogen atmosphere at room temperature. Powder x-ray diffraction (XRD) patterns of the SnO_2 NPs were recorded using a Bruker AXS D8 advanced diffractometer with Cu Kα radiation ($\lambda = 1.5406$ Å) in the range of 20–80°. The average crystallite size of the powders, d, was calculated by applying the Scherrer's equation:

$$d = \frac{k\lambda}{\beta \cos\theta}$$

where K is the shape factor taken as 0.89, λ is the wavelength of the incident beam, β is the full width at half maximum and θ is the Bragg angle.

Surface morphology, elemental and particle size analyses were done using scanning electron microscopy (SEM) equipped with energy-dispersive x-ray (EDX) analyzer (Philips XL-30-FEG) and transmission electron microscopy (JEOL 2100 F) with an accelerating voltage of 200 keV. The x-ray photoelectron spectroscopy measurements were performed using the Physical Electronics (PHI) 5800-01 high performance multi-technique analyzer with Al Kα source at a power of 350 W. The binding energies for identical samples were reproducible within ±0.10 eV. The deconvolution was carried out with peak fit software.

2.3. Preparation and analysis of real sample

Pharmaceutical folic acid tablet was chosen for FA real sample analysis (Wyeth Limited, Mumbai). The tablet was weighed and then ground to a fine powder with a mortar and pistol. The powder was mixed with 10 mL of millipore water, sonicated for 30 min and then filtered through Whatman 42 (125 mm diameter) filter paper to yield a clear solution. The solution was diluted with PB (pH 7.0) solution to the required concentration and amperometric measurement was performed using the standard addition method.

2.4. Material preparation

The synthesis process of Cu doped SnO_2 NPs was similar to our earlier report [17]. Briefly, 0.1 M solution of tin chloride dihydrate ($SnCl_2 \cdot 2H_2O$) and copper sulphate ($CuSO_4 \cdot 5H_2O$) with different Cu (0, 10 and 20wt%) content were mixed. Ammonium hydroxide (NH_4OH) was added drop wise to the above solution until the pH reached 8. This solution was stirred for 30 min to form a colloidal gel. Further, the hydroxide product was washed several times with millipore water and ethanol in order to remove the Cl^- and NH_4^+ ions respectively. Then the white colored precipitate was transferred into a microwave oven (600 W) and exposed for 20 min. Finally, the undoped and Cu doped SnO_2 NPs were obtained through annealing the precipitates at 600 °C for 5 h in an ambient atmosphere.

2.5. Fabrication of Cu doped SnO_2 NPs modified GCE

Initially, the glassy carbon electrodes were polished with 0.5 and 0.05 μm alumina slurries and then rinsed thoroughly with water. After each polishing, the electrode was sonicated in water for 5 min to remove any adhesive substances on the electrode surface. The Cu doped SnO_2 NPs modified electrode was prepared by a simple drop casting method. Typically, 5 mg of the SnO_2 NPs in millipore water (1 mL) was drop casted (10 μL) onto the GCE and air dried at room temperature for 90 min.

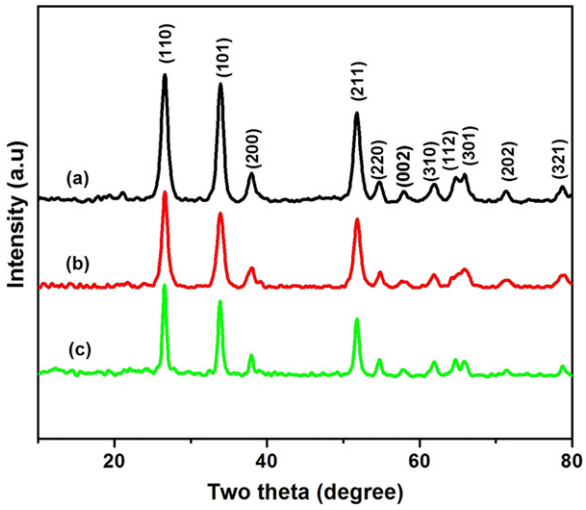

Figure 1. XRD patterns of (a) pure, (b) 10wt % and (c) 20wt% Cu doped SnO_2 NPs.

3. Results and discussion

3.1. Powder XRD and SEM analysis

The structural properties of the undoped SnO_2 and Cu (10 and 20wt%) doped SnO_2 NPs were investigated by powder XRD method. The XRD patterns (figure 1) of all the samples could be indexed to (ICDD-PDF card no. 41–1445) the rutile-type phase of SnO_2 with a tertragonal unit cell which are consistent with the standard values for bulk SnO_2. However, upon increasing the copper content, a moderate decrease in the intensity of diffraction peaks, accompanied by a pronounced broadening, has been observed. In first approximation, this can be attributed to the decrease of particle size, doping of SnO_2 with Cu through the formation of a Cu-Sn solid solution and/or to induced microstrain. Indeed, when Cu is doped into SnO_2, complicated defect-systems may form, i.e. interstitial Cu and Sn, as well as oxygen vacancy defects could exist, apart from Cu substituting Sn, through substitutional or interstitial doping. A detailed description of Cu-doping mechanism into SnO_2 structure was described earlier [18]. The XRD data of Cu-doped samples indicate that SnO_2 is still

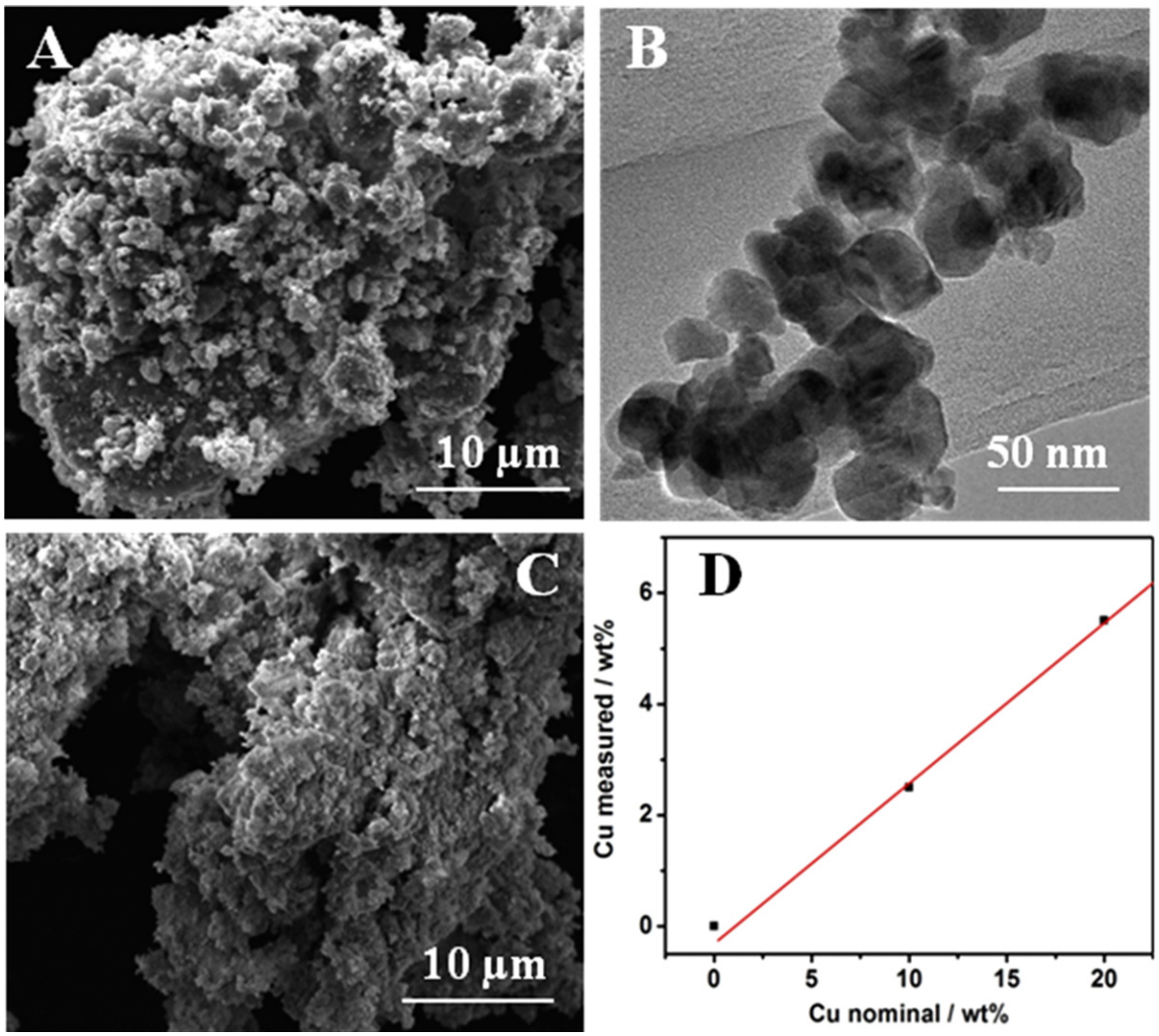

Figure 2. (A) SEM and (B) TEM images of pure SnO_2 NPs and (C) SEM image of 20wt% Cu-SnO_2 NPs. (D) Plot of nominal Cu content *vs* Cu content obtained by EDX mapping.

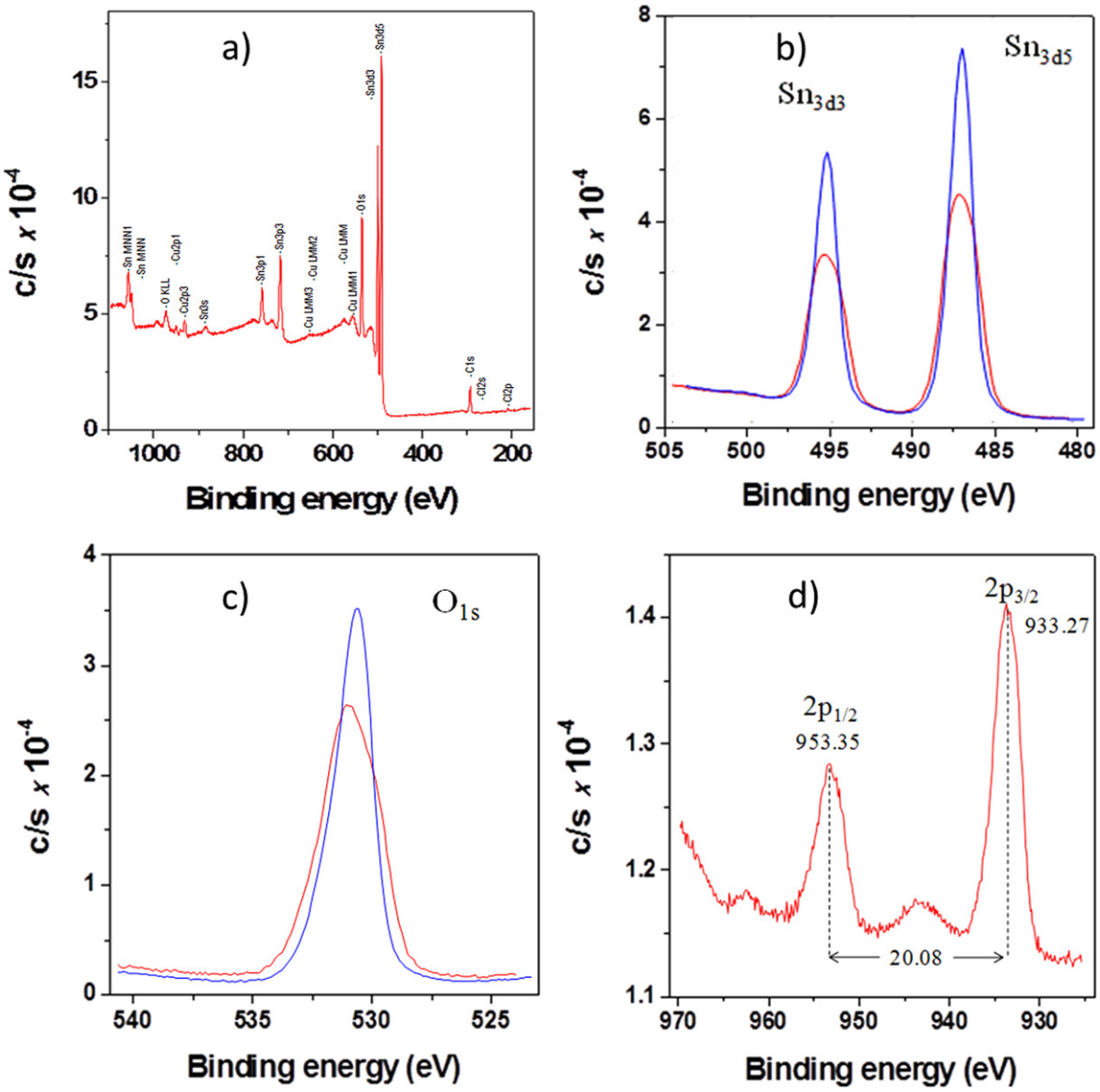

Figure 3. XPS spectra of pure and Cu (20wt%) doped SnO_2 NPs; (a) Cu-SnO_2 NPs (b) Sn3d, (c) O1s, and (d) Cu2p.

mainly in the rutile phase, suggesting a substitutional doping of Cu at Sn-site. In this case, based on the *Kroger-Vink* notations, the oxygen-ion vacancies ($V_o^{\bullet\bullet}$) created by substitutional doping of Sn^{4+} with Cu^{2+} are charge compensated by electron holes ($h^{\bullet}$), when the sample is annealed in air. A similar behavior has been also reported by Kumar *et al* [19]. However, it should be also considered that Cu could enter as 4^+ to maintain the coordination number required for rutile phase. It should be also remarked that no peaks corresponding to Cu or CuO isolated phases have been evidenced in the XRD patterns of Cu-doped SnO_2 samples, in agreement with the view that all Cu entered in the SnO_2 lattice. In this regard, it is reported that the sol-gel route leads to incorporation of high Cu^{2+} loading into the SnO_2 lattice, at least up to 10 mol% [20]. On the other hand, Santilli *et al* have evidenced the presence of only 0.7 mol% of copper in substitutional solid solution, while for higher concentration of doping, copper has been observed at the external surface of crystallites [21]. In the occurrence of this latter case, Cu isolated phases present on our samples could be in an amorphous state, not detectable by XRD. The average crystallite size evaluated by the Scherrer equation was found to be around 16 nm, 9 nm and 5 nm for pure SnO_2 and 10wt% Cu and 20wt% Cu-doped SnO_2 samples respectively, suggesting that the grain growth is suppressed due to doping of Cu into Sn-site.

Hence, SEM and EDX-mapping were carried out to investigate the nature of Cu dopant onto SnO_2 (figure 2). From these measurements we can clearly observe that the copper and tin are homogenously dispersed in the doped particles. Further, on comparing the content of Cu, obtained by EDX analysis with the nominal content, it can be noted that the experimental values are lower than nominal ones. In fact the Cu-doped samples contain roughly three times less Cu element than the expected ones (figure 2(D)). TEM image of pure SnO_2 samples (figure 2(B)) showed nearly spherical shaped nanoparticles with average particles size of 20 nm.

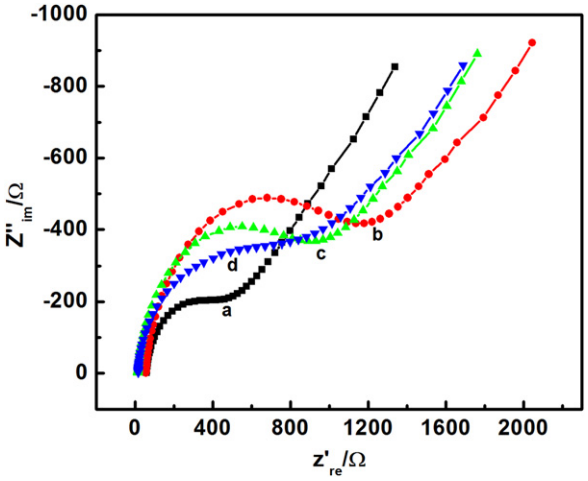

Figure 4. Electrochemical impedance behavior of the modified GCE measured in the frequency region from 0.1 Hz to 100 kHz at the dc potential 250 mV and ac potential ±5 mV in presence of 1 mM $[Fe(CN)_6]^{3-/4-}$ containing 0.1 M KCl; (a) bare GC, (b) pure SnO_2, (c) 10wt% and (d) 20wt% Cu doped SnO_2 NPs.

3.2. XPS analysis

Figure 3(a) shows XPS spectrum of the 20wt% Cu doped SnO_2 sample which clearly show photoelectronic lines of Sn and Cu. Figures 3(b)–(d) show Sn-3d, O–1s and Cu-2p core level regions of the same sample. A doublet at 487.2 and 495.5 eV can be assigned to Sn $3d_{5/2}$ and $Sn3d_{3/2}$ respectively which indicates that the Sn atoms are in 4^+ state and the Cu doping does not change its valence state [22]. The peak intensity of Cu-SnO_2 NPs was found to be lower as compared to that of pure SnO_2 which could be attributed to the reduced particle size due to Cu-doping. The O1s peaks are located at 530.3 eV and 531.5 for pristine and Cu (20wt%) doped SnO_2 samples, which corresponds to O^{2-} ions in SnO_2 lattice. The Cu-2p binding energy region is shown in figure 3(d). Photoelectron peaks corresponding to the Cu 2p3/2 and 2p1/2 core levels were observed at 933.3 and 953.3 eV with a separation of 20.1 eV which is identified as the binding energy of Cu^{2+}. The two satellite peaks (S1, S2) centered at 942.8 and 962.5 eV are characteristics of Cu^{2+}. The results suggest that the Cu ions are successfully substituted in the tetragonal rutile SnO_2 lattice without forming any detectable impurity phase such as Cu or Cu_2O.

3.3. EIS characterization of Cu-SnO_2 NPs modified GC electrode

Figure 4 shows the impedance spectra obtained for bare GC, pure SnO_2, 10wt% and 20wt% Cu doped SnO_2 NPs modified GC electrodes in $[Fe(CN)_6]^{3-/4-}$ containing 0.1 M KCl at scanning frequencies from 0.1 to 100 KHz. The obtained complex plane plots (Nquist plots) for the imaginary component of impedance against its real component (Z''_{im} *vs* Z'_{re}) were best fit with the Randles equivalent circuit model [Rs (Q_{CPE}(R_{ct}W))] for bare GC, undoped SnO_2, and Cu doped SnO_2 (10 & 20wt%) modified electrodes using Zsimpwin software. In this model, R_s is solution resistance, Q_{CPE} is constant phase element, and W is the Warburg diffusion coefficient. The value of the charge transfer resistance (R_{ct}) for the bare GC, pure SnO_2, 10wt% and 20wt% Cu doped SnO_2 modified GC electrodes were estimated as 380, 1015, 820 and 690 $\Omega\,cm^2$ respectively. The R_{ct} value of 20wt% Cu doped SnO_2 modified GC electrode is nearly 1.5 and 1.2 fold lower than that of the undoped SnO_2 and the 10wt% Cu doped SnO_2 NPs modified GC electrodes respectively. It may due to the uniform distribution of Cu on SnO_2 as evidenced from SEM and EDX measurements. In addition, smaller particle size (5 nm) of 20wt% Cu-SnO_2 might have facilitated the redox reaction of $[Fe(CN)_6]^{3-/4-}$.

3.4. Electrocatalytic activity of the Cu-SnO_2 modified electrode towards FA

Figure 5(A) shows the CVs obtained for 1.0 mM FA at bare GC (curve a), pure SnO_2 (curve b) 10wt% (curve c) and 20wt% (curve d) Cu doped SnO_2 NPs modified GC electrodes in 0.1 M PB solution (pH 7.0). Compared to those obtained at the bare GC (11 μA), pure SnO_2 (12 μA), 10wt% Cu-SnO_2 (13 μA), a fairly larger peak current was obtained at the 20wt% Cu-SnO_2 (15 μA) modified GC electrode. This result suggested that the electron transfer reaction at the 20wt% Cu-SnO_2 based electrode is more facile than that at the bare GC, pure SnO_2 and 10wt% Cu-SnO_2 modified GC electrodes. It is also noted that the 20wt% Cu-SnO_2 modified electrode show an oxidation peak potential at 0.76 V, which is 40 mV less than that was observed for bare GC electrode. At the same time, this electrode did not show any oxidation peak in the absence of FA (figure 5(B), curve a). Further, the effect of scan rates on the oxidation of FA at 20wt% Cu-SnO_2 electrode for scan rates from 50–500 mV s^{-1} in 0.1 M PB (pH 7.0) solution is shown in figure 5(C). A good linearity was obtained while plotting the current against square root of scan rate with correlation coefficients of 0.9995 (inset of figure 5(C)) indicating that the oxidation of FA at the Cu-SnO_2 modified electrode was a diffusion controlled process. Further it involves two electron oxidation of FA to dehydrofolic acid at the Cu-SnO_2 modified GC electrode as represented in the following reaction.

Figure 6 shows the linear sweep voltammograms (LSVs) obtained for FA in the concentration range of 0–100 μM at the Cu-SnO_2 modified electrode. The oxidation peak current of FA got enhanced with the increase in FA concentration (each step with the increment of 5 μM). The oxidation current has a linear relationship with concentration of FA with a correlation coefficient of 0.998 (inset of figure 6).

3.5. Determination of folic acid by amperometry and DPV

Amperometric method was used to examine the sensitivity of the Cu-SnO_2 modified GC electrode towards the detection of FA. Figure 7 shows the amperometric *i-t* curve for FA at Cu-SnO_2 modified electrode in a homogeneously stirred 0.1 M PB solution (pH 7.0) under the applied potential of 0.8 V. The modified electrode shows the initial current response due to 100 nM FA. The current response increases and a steady state

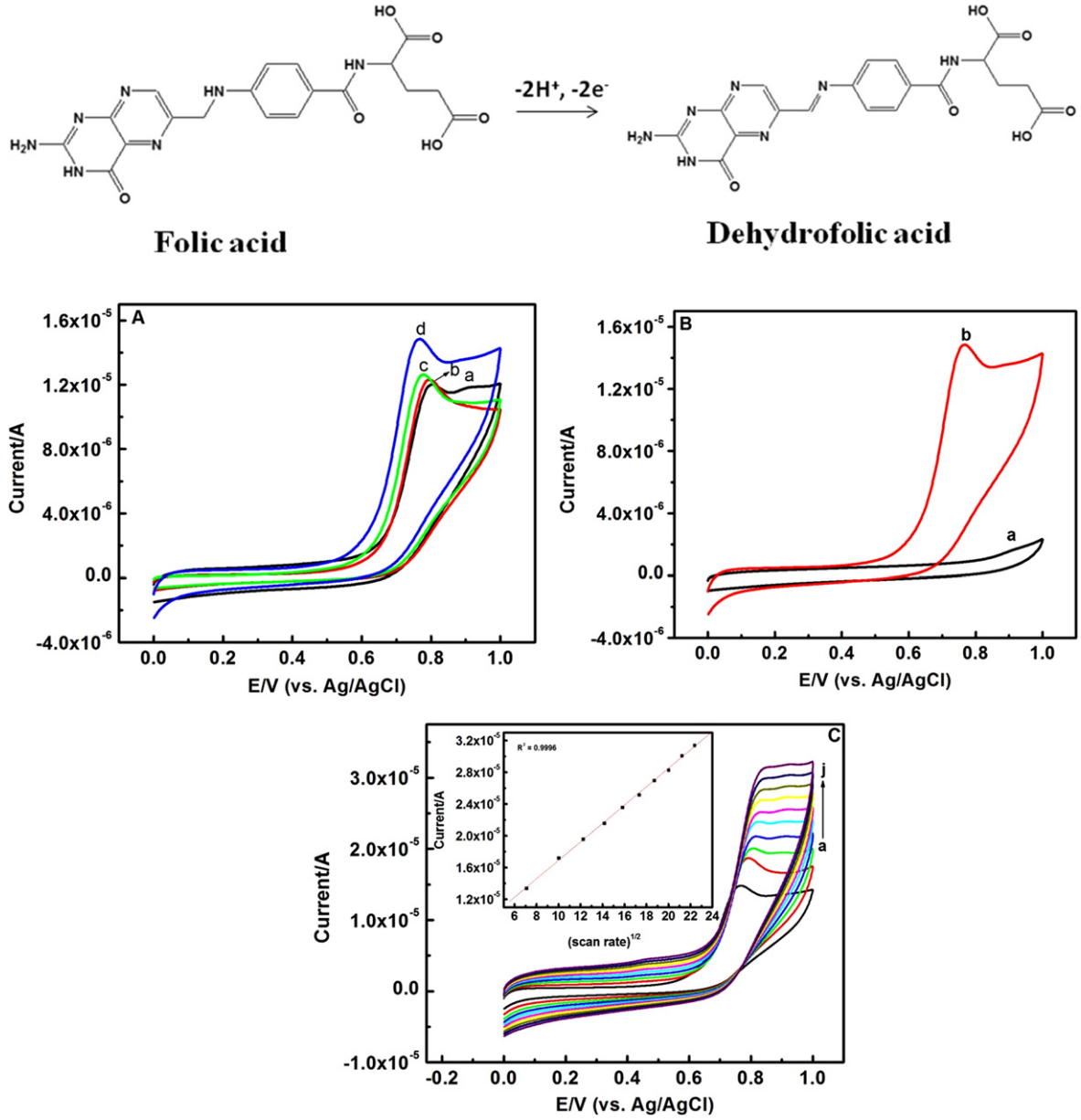

Figure 5. (A) CVs obtained for 1 mM FA at the (a) bare GC, (b) SnO_2, (c) 10wt% Cu-SnO_2 and (d) 20wt% Cu-SnO_2 modified electrodes in 0.1 M PBS (pH 7.0). (B) CVs obtained at 20wt% Cu-SnO_2 (a) in the absence and (b) presence of 1 mM FA in 0.1 M PBS (pH 7.0). (C) CVs obtained for 1 mM FA at 20wt% Cu-SnO_2 modified GC electrode in 0.1 M PBS at different scan rates; (a) 50, (b) 100, (c) 150, (d) 200, (e) 250, (f) 300, (g) 350, (h) 400, (i) 450 and (j) 500 mV s^{-1}. Inset: plot of the anodic peak current *vs* square root of scan rate.

current response were attained within 5 s for further addition of 100 nM FA in each step with a sample interval of 100 s. The dependence of response current with respect to concentration of FA was linear from 100 nM to 900 nM at Cu-SnO_2 modified electrode with a correlation coefficient of 0.998 (inset of figure 7). Further, the amperometric current response increased linearly with increasing FA concentration in the range of $1.0\times10^{-7}-4.0\times10^{-4}$ M with a correlation coefficient of 0.992 and the detection limit was found to be 7.2×10^{-8} M.

Figure 8 displays the DPV response of FA in the optimized working conditions for the fabricated electrode. A linear relationship could be observed between i_{pa} and the concentration of FA in the range from 1.0×10^{-10} to 6.7×10^{-5} M with the lowest detection limit of 2.4×10^{-11} M. The sensing characteristics of the Cu-SnO_2 modified GC electrode are very much comparable with that of the literature for similar modified electrodes (table 1). Moreover, the fabricated sensor has several advantages like (i) simple and speedy preparation of sensing material Cu-SnO_2 NPs, (ii) the detection of FA in physiological pH, (iii) the fabrication of the modified electrode in a short time and (iv) high stability and reproducibility.

3.6. Effect of interferents on the behavior of FA

It is well known that the ascorbic acid coexists with FA in human body fluid and its concentration is always much higher

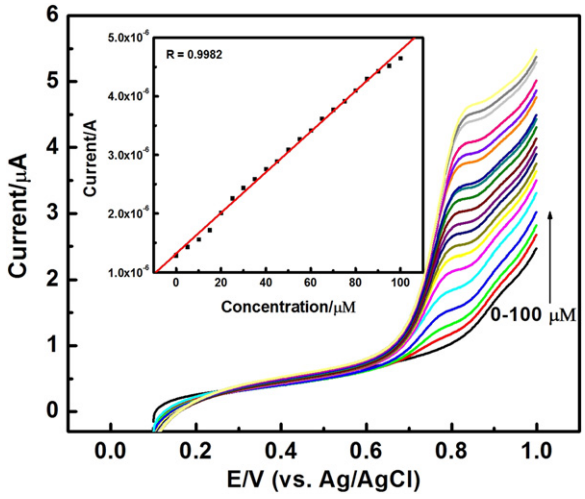

Figure 6. LSVs obtained for FA in the concentration ranging from 0 to 100 μM. FA was added in steps of 5 μM each at the Cu-SnO_2 modified electrode in PBS (pH 7.0).

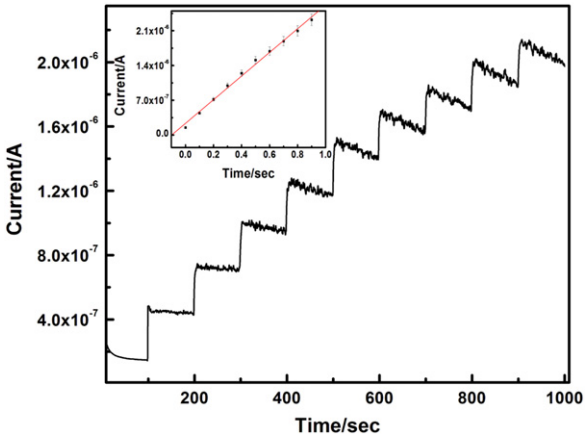

Figure 7. Amperometric *i-t* curve for the determination of FA at Cu-SnO_2 modified GC electrode in 0.1 M PB solution (pH 7.0). 100 nM of FA was added at each step at the time interval of 100 s (E_{pa} = 0.80 V).

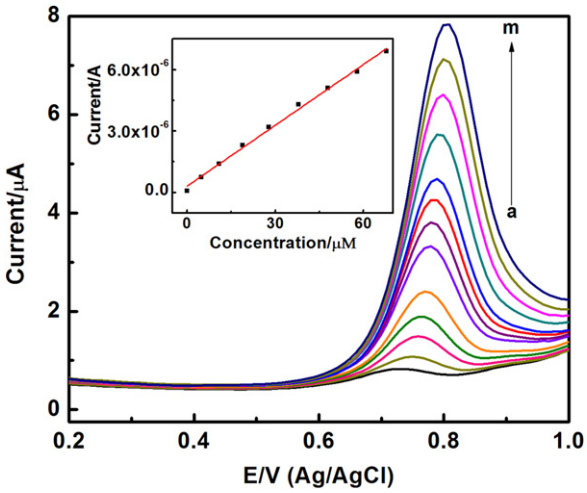

Figure 8. DPVs recorded for Cu-SnO_2/GCE in 0.1 M PBS with various concentration of FA (a-m: 1.0×10^{-10} to 6.7×10^{-5} M) under amplitude = 0.05 V and pulse period 0.05 s.

than that of FA. Therefore the determination of FA in the presence of high concentration of AsA is very important. Voltammetric response of FA in the presence of a large excess of AsA was tested by DPV in pH 7.0 phosphate buffer (figure 9(A)). The oxidation peak current of FA increased with varying concentration from 10–50 μM while AsA current was decreased. The presence of 100-fold excess of AsA did not bring any effect on the responses of FA which confirmed the selective determination of FA by the fabricated sensor. Further the anti-interference ability was tested by amperometry through introducing electroactive species such as glucose, lactose, urea, riboflavin, NaCl and KCl (figure 9(B)). It was found that the presence of 5 fold excess of the above species did not interfere with the measurement of folic acid which again confirmed that the proposed sensor is free from the most common interferents.

3.7. Stability and reproducibility of Cu-SnO_2 electrode

In order to investigate the stability of the Cu-SnO_2 electrode, the amperometric responses for 5.0 μM FA in 0.1 M PBS (pH 7.0) was recorded for every 60 min interval. It was found that the oxidation current remained nearly the same with a relative standard deviation of 2.73% for 4 times repetitive measurements which indicates that the electrode has a good reproducibility.

The fabricated Cu-SnO_2 based electrode was kept in closed air atmosphere at room temperature after amperometric measurements. The current response of the modified electrode got decreased by about 2.1% in 1 week and 4.5% in about 2 weeks. To ascertain the reproducibility of the results further, three different GC electrodes were modified with the Cu-SnO_2 and their responses towards an oxidation of 0.5 μM FA were tested. The amperometric current obtained in the measurements of three independent electrodes (1.46, 1.62 and 1.45 μA) showed a relative standard deviation of 6.32% confirming that the results are reproducible. The above results showed that the Cu-SnO_2 based electrode was very much stable and reproducible towards folic acid analyte.

3.8. Determination of FA in pharmaceutical sample

The practical application of the Cu-SnO_2 electrode was tested by measuring the concentration of FA in pharmaceutical tablet with standard addition method. The results (table 2) show that the newly fabricated biosensor is useful to measure folic acid in pharmaceutical samples.

4. Conclusion

We have successfully synthesized Cu (10, 20wt%) doped SnO_2 NPs by microwave irradiation method and demonstrated that the Cu-SnO_2 modified GCE offers a good, reliable and simple method for the selective determination of FA at pH 7.0. The Cu-SnO_2 modified electrode not only shifted the oxidation potential of FA towards less positive potential but

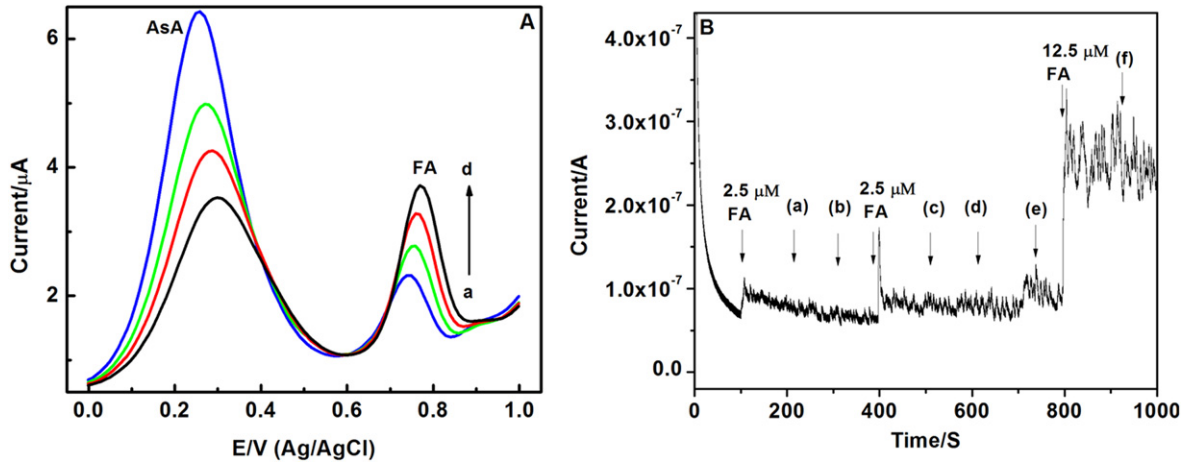

Figure 9. (A) DPVs obtained for the increment of FA from 10–50 μM in the presence of 1000 μM ASA in 0.1 M PBS at Cu-SnO_2 modified GC electrode. (B) Amperometric response of the Cu-SnO_2 modified electrode for the addition of FA and successive additions of interferents (12.5 μM) in the sequence of (a) glucose, (b) NaCl, (c) lactose, (d) KCl, (e) riboflavin and (f) urea in 0.1 M PB solution.

Table 1. Comparison of the detection limit of FA sensing by various modified electrodes.

Electrodes	Method	pH	Linear range (μM)	Detection limit (μM)	Reference
DNA-PGE	DPV	4.8	0.1–10	0.0106	[9]
α Fe_2O_3	i-t curve	7.0	0.06–60	0.000 112	[10]
MWCNTs-PBCB	DPV	7.0	900–2310	96	[11]
SWCNT	CV	5.5	0.01–100	0.001	[12]
ZrO_2-CPE	DPV	7.0	20–2500	9.86	[23]
Polymer immobilized sol-gel PEG	DPCSV	2.5	20–300	0.005	[24]
p-AMT	i-t curve	7.2	0.1–800	0.0002	[25]
PMo_{12}-PPy	DPV	<3.0	0.01–0.1	0.0001	[26]
Ni-POA/CPE	CV	13	100–5000	91	[27]
MWCNT	ASV	6.4	0.3–80	0.13	[28]
Cu-SnO_2	DPV	7.0	0.01–67	0.000 024	Present work

Table 2. Determination of FA in pharmaceutical sample using Cu-SnO_2 electrode.

Samples	Labelled content (mg/tablet)	Observed Content (mg/tablet))	Recovery%
Folvite	5	4.968	98.3
Foligen	5	4.842	100.1

also enhanced its oxidation current when compared to undoped SnO_2 modified and bare GC electrodes. The DPV current increased linearly while increasing the concentration of FA from 1.0×10^{-10} to 6.7×10^{-5} M with the lowest detection limit of 2.4×10^{-11} M. The practical application of the fabricated electrode was demonstrated in pharmaceutical tablet by the recovery test. All these advantageous features make the proposed Cu-SnO_2 nanoparticles based FA biosensor applicable in food, pharmaceutical and other relevant areas.

Acknowledgement

Authors NL & CS acknowledge the University Grants Commission (UGC. F. No. 40-2/2011) and Council of Scientific and Industrial Research (CSIR No.03(1203)/12/EMR-II) for the financial assistance.

References

[1] Bates C J 2003 *Encyclopedia of Food Sciences and Nutrition* 2nd edn (New York: Academic) pp 2559–64
[2] McRae M P 2009 *J. Chiropractic Medicine* **8** 15–24
[3] Breithaupt D E 2001 *Food Chem.* **73** 521–5
[4] Pawlosky R J and Flanagan V P 2001 *J. Agric. Food. Chem.* **49** 1282–6
[5] Kanjilal G, Mahajan S N and Rao G R 1975 *Analyst* **100** 19–24
[6] Zhang B T, Zhao L and Lin J M 2008 *Talanta* **74** 1154–9
[7] Blanco C C, Carretero A S, Gutierrez A-F and Ceba M-R 1994 *Anal. Lett.* **27** 1339–53
[8] Home D W and Patterson D 1988 *Clin. Chem.* **34** 2357–9

[9] Mirmoghtadaie L, Ensafi A A, Kadivar M and Norouzi P 2013 *Mat. Sci. Eng.* C **33** 1753–8
[10] Maiyalagan T, Sundaramurthy J, Suresh Kumar P, Kannan P, Opallo M and Ramakrishna S 2013 *Analyst* **138** 1779–86
[11] Umasankar Y, Ting T W and Chen S M 2011 *J. Electrochem. Soc.* **158** K117–22
[12] Chenghang W, Chunya L, Ting L, Xiuling X and Changfa W 2006 *Microchim Acta* **152** 233–8
[13] Gopel W and Schierbaum K D 1995 *Sens. Actuators* B **26** 1–12
[14] Li L, Huang J, Wang T, Zhang H, Liu Y and Li J 2010 *Biosens. Bioelectron.* **25** 2436–41
[15] Lavanya N, Radhakrishnan S and Sekar C 2012 *Biosen. Bioelectron.* **36** 41–7
[16] Selvan R K, Perelshtein I, Perkas N and Gedanken A 2008 *J. Phys. Chem.* C **112** 1825–30
[17] Lavanya N, Radhakrishnan S, Sekar C, Navaneethan M and Hayakawa Y 2013 *Analyst* **36** 2061–7
[18] Ghimbeua C M, Van Landschoot R C, Schoonman J and Lumbreras M 2010 *J. Eur. Ceram. Soc.* **27** 207–13
[19] Kumar V, Sen S, Muthe K P, Gaur N K, Gupta S K and Yakhmi J V 2009 *Sens. Actuators* B **138** 587–90
[20] Davis R, Chadwick A V and Wright J D 1997 *J. Phys. Chem.* B **101** 9901–8
[21] Santilli C V, Pulcinelli S H, Brito G-E S and Briois V 1999 *J. Phys. Chem.* B **103** 2660–7
[22] Hong Z S, Cao Y and Deng J F 2002 *Mater. Lett.* **52** 34–8
[23] Ardakani M M, Beitollahi H, Amini M K, Mirkhalaf F and Alibeik M A 2010 *Sens. Actuators* B **151** 243–9
[24] Prasad B B, Madhuri R, Tiwari M P and Sharma P S 2010 *Sens. Actuators* B **146** 321–30
[25] Kalimuthu P and John S A 2009 *Biosens. Bioelectron.* **24** 3575–80
[26] Guo H X, Li Y Q, Fan L F, Wu X Q and Guo M D 2006 *Electrochim. Acta* **51** 6230–7
[27] Ojani R, Rahoof J B and Zamani S 2009 *Electroanal.* **21** 2634–9
[28] Jiang X L, Li R, Li J and He X 2009 *Russ. J. Electrochem.* **45** 772–7